This is the accepted manuscript made available via CHORUS. The article has been published as:

Generation of a Cat State in an Optical Sideband

Takahiro Serikawa, Jun-ichi Yoshikawa, Shuntaro Takeda, Hidehiro Yonezawa, Timothy C. Ralph, Elanor H. Huntington, and Akira Furusawa

Phys. Rev. Lett. **121**, 143602 — Published 4 October 2018

DOI: 10.1103/PhysRevLett.121.143602

Generation of Cat State in an Optical Sideband

Takahiro Serikawa,[1] Jun-ichi Yoshikawa,[1] Shuntaro Takeda,[1] Hidehiro Yonezawa,[2,3]
Timothy C. Ralph,[3,4] Elanor H. Huntington,[3,5] and Akira Furusawa[1*]
[1]*Department of Applied Physics, School of Engineering,*
The University of Tokyo, 7-3-1 Hongo, Bunkyo-ku, Tokyo, Japan.
[2]*School of Engineering and Information Technology, The University of New South Wales, Canberra, ACT 2600, Australia*
[3]*Center for Quantum Computation and Communication Technology, Australian Research Council, Australia.*
[4]*School of Mathematics and Physics, University of Queensland, Brisbane, QLD 4072, Australia. and*
[5]*Research School of Engineering, College of Engineering and Computer Science,*
Australian National University, Canberra, ACT 2600, Australia.
(Dated: August 29, 2018)

We propose a method to subtract a photon from a double sideband mode of continuous-wave light. The central idea is to use phase modulation as a frequency sideband beamsplitter in the heralding photon subtraction scheme, where a small portion of the sideband mode is downconverted to 0 Hz to provide a trigger photon. An optical cat state is created by applying the proposed method to a squeezed state at 500MHz sideband, which is generated by an optical parametric oscillator. The Wigner function of the cat state reconstructed from a direct homodyne measurement of the 500 MHz sideband modes shows the negativity of $W(0,0) = -0.088 \pm 0.001$ without any loss corrections.

Implementation of quantum operations or creation of quantum states on multiplexed photonic modes is a key for universal and scalable photonic quantum information processing (QIP). Time-division or frequency-division multiplexing provides the means of compact generation and manipulation of numerous quantum states. Recent demonstrations of large-scale continuous-variable (CV) cluster states [1] in time [2] and frequency [3, 4] domains are excellent examples of multiplexed quantum optics, though they belong to Gaussian states and transformations. Employing the cluster states, CV one-way quantum computing model [5, 6] offers a framework of QIP, where ancillary non-Gaussian states or measurements are required for its universality [6–8].

Photon subtraction [9, 10] is a common method to create non-Gaussian states, and has been established on baseband photonic modes. It is a versatile technique and has wide applications, such as quantum noiseless amplification [11], entanglement enhancement [12, 13], or a creation of particle-wave hybrid entanglement [14]. An optical cat state is a famous example of non-Gaussian states created by means of subtracting a photon from a squeezed vacuum state [15–17]. Cat states are powerful resources to implement several applications of QIP such as quantum error correction [18, 19] or quantum computing based on coherent states [20]. Incorporating frequency-domain techniques in the photon subtraction scheme will lead to universal and practical quantum operations over multiplexed photonic modes [21–25].

High-frequency sideband modes are desirable target of the frequency-division multiplexing, since such modes can be broadband. The bandwidth is practically important, especially when they are combined with the time-domain techniques such as time-bin encoding [26, 27] or time-domain cluster state computation [2, 6]. Here, to access a certain optical mode at high-frequency sideband for photon subtraction, we need to selectively tap off and detect a photon in the target mode. This is a challenging task because sideband modes are sinusoidal waves on an optical beam and higher frequency modes require higher timing resolution to be addressed.

In this Letter, we propose a method to do photon subtraction in a manner that can be easily extended to creation of multiple non-Gaussian states on high-frequency modes of a single laser beam. For the basis of the subtraction process, an optical double sideband (DSB) mode, i.e., a balanced superposition of upper and lower sideband modes around a carrier frequency, is employed. The proposed method is experimentally applied to a squeezed state generated by an optical parametric oscillator (OPO). A cat state is heralded on the 500.6 MHz DSB mode. The bandwidth of the created cat state is about 5 MHz which is comparable to that of the conventionally demonstrated optical non-Gaussian state generation. State verification is done by homodyne tomography and the cat state has excellent negativity in the Wigner function. The negativity is directly measured on the high-frequency sideband without loss correction, showing that the quantum non-Gaussianity can be actually used for applications that include measurement and feedforward, such as one-way quantum computing.

A DSB mode is described as $\left(e^{i\theta}\hat{a}_\Omega + e^{-i\theta}\hat{a}_{-\Omega}\right)/\sqrt{2}$, where $\hat{a}_\Omega$ is an annihilation operator at frequency Ω around the carrier frequency, and θ is an arbitrary phase. In time-domain, it has a real, sinusoidal envelope $\cos(\Omega t + \theta)$. To access DSB modes, phase or amplitude modulation can be used; for example displacement operations has been implemented on DSB modes by a modulator and a beamsplitter. Since DSB modes are apart of the carrier frequency, they are free from the technical noise of the carrier, which enables shot-noise-limited measurement of the field amplitude, leading to, for example, an atomic quantum memory of a DSB light realized by measurement and feedback [28]. Here, corresponding to two degrees of freedom of $\hat{a}_\Omega$ and $\hat{a}_{-\Omega}$, DSB modes at frequency Ω are decomposed into two quadrature phase components, namely, *cos-sideband* $\hat{a}_\Omega^{\cos} = \left(\hat{a}_\Omega + \hat{a}_{-\Omega}\right)/\sqrt{2}$ and *sin-sideband* $\hat{a}_\Omega^{\sin} = \left(\hat{a}_\Omega - \hat{a}_{-\Omega}\right)/\sqrt{2}i$. Thus dealing with DSB modes is

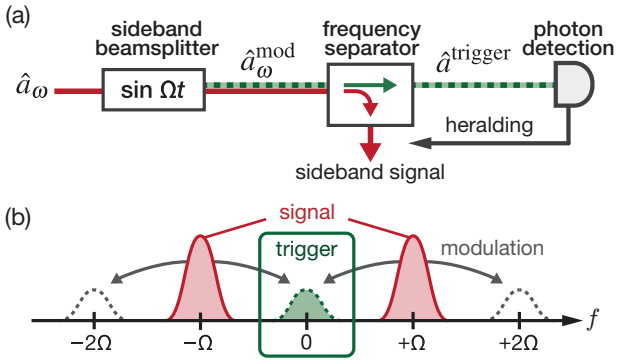

FIG. 1. (a) Schematics of photon subtraction from a double sideband. (b) Frequency diagram. A phase modulation with the signal $\sin \Omega t$ is applied to the input light. The cos-sideband component is coupled to the trigger mode at 0 Hz, which is initially prepared as a vacuum state. The trigger mode is spatially separated from the sideband signal and guided to the photon detector. The arrival of a trigger photon heralds photon subtraction from the sideband.

always a multi-mode problem; photon subtraction should selectively access one of them.

The concept of our method is depicted in Fig. 1. A small portion of the signal light at frequency Ω is downconverted to 0 Hz by a *sideband beamsplitter*. This is realized by a small phase modulation, which transfers an optical component at a given frequency to both upper and lower sidebands [29]. In the Heisenberg picture, weak frequency-Ω modulation transforms $\hat{a}_\omega$ for $\omega \in \mathbb{R}$ as

$$\hat{a}_\omega^{\mathrm{mod}} \sim \sqrt{1-\frac{\beta^2}{2}}\hat{a}_\omega + \frac{\beta}{2}\left(e^{i\theta}\hat{a}_{\omega+\Omega} + e^{-i\theta}\hat{a}_{\omega-\Omega}\right), \quad (1)$$

where $\beta \ll 1$ expresses the modulation depth and θ is determined by the modulation phase. This creates a superposition of upper and lower sidebands at 0 Hz, while some part of Ω-sideband component is transferred to 2Ω-sideband. In this way, trigger photons are prepared at 0 Hz just in a single optical beam, which is simpler implementation than a straightforward way of making a superposition of upper and lower frequency, such as a combination of frequency separation, frequency shift and interference by a beamsplitter. The frequency separator passes the 0 Hz component to the trigger line, while the signal light at $\pm\Omega$ is spatially extracted from it. Subsequent photon detection heralds a photon subtraction event, which can be expressed as conditioning by a single-photon state of the trigger mode as

$${}_{\mathrm{trigger}}\langle 1| \sim {}_{\mathrm{sig}}\langle 0|\left[\hat{a}_0 + \frac{\beta}{\sqrt{2}}\frac{e^{i\theta}\hat{a}_\Omega + e^{-i\theta}\hat{a}_{-\Omega}}{\sqrt{2}}\right], \quad (2)$$

where the creation operator of the trigger mode is reduced to the signal modes by Eq. (1). Since the initial state of $\hat{a}_0$ is assumed to be vacuum, the conditioning with Eq. (2) results in photon subtraction on the DSB mode with the phase θ, which can be controlled by tuning the modulation phase.

Note that the effect of the finite linewidth of the separator is ignored here. Actually, a photon is subtracted from a wavepacket as conventional baseband subtraction methods; see Supplement Material for a further formulation.

A significant advantage of the DSB basis is that highly-multiplexed, potentially over thousands of, squeezed vacuum states in DSB modes are available by a continuously-pumped optical parametric oscillator (OPO) [4, 30]. The photon-pair generation process of a degenerate OPO is described by $\exp\left(\int_0^\infty d\omega\, r(\omega)\,\hat{a}_\omega^\dagger \hat{a}_{-\omega}^\dagger - \mathrm{h.c.}\right)$ where $r(\omega)$ denotes the squeezing spectrum, which has comb-like shape corresponding to the resonances of the OPO. With the DSB basis, this is reinterpreted as two photon creation / annihilation process of each DSB mode since $\hat{a}_\omega^\dagger \hat{a}_{-\omega}^\dagger = \left[(\hat{a}_\omega^{\cos\dagger})^2 + (\hat{a}_\omega^{\sin\dagger})^2\right]/2$. Thus we have independent squeezed states on both sin- and cos-sideband modes, which include even thousands of frequency combs [31] and can be used for the resource of non-Gaussian state generation.

Figure 2(a) shows the experimental setup. A cat state is created by subtracting a photon from a squeezed vacuum state at a DSB mode, which is prepared by an OPO. We carefully identify the free spectral range (FSR) of the OPO at $2\Omega = 1001.2\,\mathrm{MHz}$ to determine the sideband frequency $\Omega = 500.6\,\mathrm{MHz}$. Our OPO is resonant at $(2n+1)\Omega$, $n \in \mathbb{Z}$ with the linewidth of 10 MHz, while it is anti-resonant at 0 Hz providing vacuum state there. Since the squeezing operation of the OPO can be factorized in the sin- and cos-sideband modes, the squeezed state is separable in the DSB basis. When we only look at 0 Hz mode and the first resonance at Ω, the output of the OPO is expressed as

$$|\Psi_0\rangle = |0\rangle_0 \otimes \hat{S}_r|0\rangle_{\cos} \otimes \hat{S}_r|0\rangle_{\sin}, \quad (3)$$

where $|0\rangle_0$ is a vacuum state of $\hat{a}_0$ and $\hat{S}_r|0\rangle_{\cos,\sin}$ are squeezed states of $\hat{a}_\Omega^{\cos}$ and $\hat{a}_\Omega^{\sin}$, respectively. For the simplicity, we omit the multi-mode description of the continuous-wave squeezed light here; again, see Supplemental Material.

In order to apply phase modulation at 500.6 MHz without inducing decoherence, we use a bulk electro-optic modulator (EOM) that has low-optical loss below 0.5%. The transfer efficiency β^2 is set at 0.040. By adjusting the phase of the driving signal of the EOM, cos-sideband mode is selectively downconverted to 0 Hz, i.e., θ in Eq. (1) is set at zero. The frequency separator consists of three optical cavities, and extracts the trigger photon component at 0 Hz with about 5 MHz of bandwidth, while rejecting all the higher frequency resonances of the OPO over several hundred GHz. The clicks of the avalanche photodiode (APD) provide the trigger signal for photon subtraction. Applying Eq. (2) on Eq. (3) yields a cat state in the cos-sideband mode, while the sin-sideband mode remains as a squeezed vacuum state:

$$|\Psi_{\mathrm{cat}}\rangle \propto {}_{\mathrm{trigger}}\langle 1|\Psi_0\rangle \propto \hat{a}_\Omega^{\cos}\hat{S}_r|0\rangle_{\cos} \otimes \hat{S}_r|0\rangle_{\sin}. \quad (4)$$

The cat state actually has a wavepacket-like envelope $\xi(t)$ and is generated in a sideband wavepacket $\cos\Omega t\,\xi(t-\tau)$ around the trigger time τ. The shape of the envelope is determined by the frequency characteristics of the squeezed state and the transmission spectrum of the frequency separator, which are

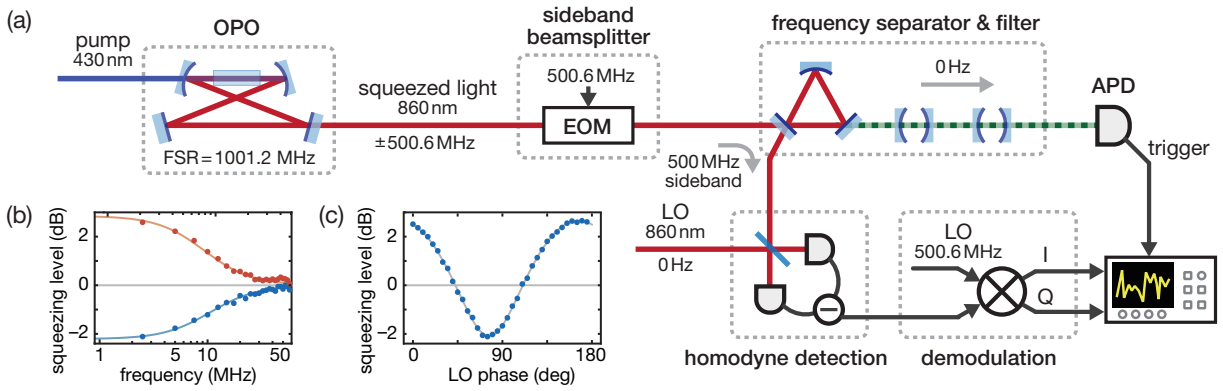

FIG. 2. (a) Schematic of the experiment. I and Q denote in-phase and quadrature component of the homodyne signal. (b) Squeezing / anti-squeezing spectrum around the 500.6 MHz sideband. The power spectrum is calculated by fast Fourier transformation of the homodyne detection. This is an average of 8000 traces of 400 ns period, and normalized by the shotnoise power. (c) Phase scan plot of the low-frequency squeezing level. Theoretical curves are also shown.

tunable parameters and in principle can be matched to external devices such as optical memories.

The quadrature distributions of the sin- and cos-sideband modes are measured by homodyne detection with a continuous-wave optical local oscillator (LO) at 0 Hz. 83% of effective detection efficiency is realized at 500 MHz by a low-loss, low-noise resonant homodyne detector [32]. The two DSBs are electrically resolved by a demodulator with a pre-defined electrical LO at frequency Ω, giving cos- and sin-sideband quadrature as in-phase and quadrature-phase output.

Figure 2(b) shows the squeezing spectrum at the 500.6 MHz sideband calculated from the quadrature-phase component (sin-sideband mode) of the homodyne detection. We obtain 2.2 dB of squeezing and the total efficiency of sin-sideband is estimated at $\eta^{\sin} = 0.70$. Figure 2(c) is the phase scan plot of the squeezing level averaged within DC-5 MHz. The squeezing phase is estimated at 66 degrees. The phase of the squeezed state can be easily changed by adjusting the pump phase locking.

For the tomography of the cat state, the in-phase (cos-sideband) and quadrature (sin-sideband) signals are simultaneously digitized with the trigger signals. 8,000 samples of quadrature signals for each 36 equally partitioned optical phases are collected.

The envelope function $\xi(t)$ of the cat states are identified by independent component analysis [33] of the demodulated cos-sideband waveforms and shown in Fig. 3. The estimated $\xi(t)$ has about 5 MHz of bandwidth, and well matches the theoretical curve, which is obtained as a convolution of the correlation function of the OPO and the impulse response of the trigger line filters. Since the bandwidth of the trigger line filters is narrower than that of the OPO, the envelope function resembles the single-sided decay function of the filter's response. The quadrature of the wavepacket of a cat state is given by a weighted integration of in-phase signal with $\xi(t)$, which is realized by a digital filter and the impulse response of the homodyne detector (see Supplemental Material). In order to discuss the sideband-selectivity of our method, we also extract the quadrature of the sin-sideband wavepacket that has the same envelope as the photon-subtracted state.

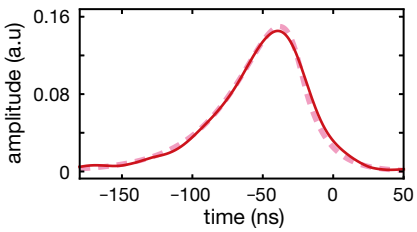

FIG. 3. Estimated envelope function $\xi(t)$ of the sideband wavepacket of the subtracted mode. The time origin is placed at the trigger time. The dashed line shows the theoretical curve.

The quadrature distributions of cos- and sin-sideband wavepacket modes show the effect of subtraction (Fig. 4(a)), where only the cos-sideband state is reshaped by the conditions of the triggers. The non-classical nature of the generated state is confirmed by the negativity of the Wigner function obtained by maximum-likelihood estimation [34] (Fig. 4(b)). The cos-sideband state shows $W_{\cos}(0,0) = -0.088 \pm 0.001$ ($\hbar = 1$) without loss correction, which is to be compared with the negative peak of the pure cat states $W_{\mathrm{cat}}(0,0) = -1/\pi$. The fidelity of the cos-sideband state to the best-fit minus cat state $|\Psi\rangle = \mathcal{N}\big[|\alpha\rangle - |-\alpha\rangle\big]$, with the coherent state amplitude $\alpha = 0.88 - 0.19i$, is 64%. Both optical losses and contamination from the sin-sideband contribute to $W(0,0)$ as a mixture of plus value $1/\pi$. In this sense, when the estimated total efficiency $\eta^{\cos} = 0.68$ (see Supplemental Material) is considered, we expect $W_{\cos}(0,0) = -0.114$. To fit the actual value of $W_{\mathrm{cat}}(0,0)$, 4% of the mixture of background squeezed state is presumed where the fake clicks of the APD and the impurity from the inherent mode-mismatch of photon subtraction [35] contributes 0.8% and 3.0% to it respectively. Thus the upper bound of the mixture of the sin-sideband component is estimated below 1%. The sin-sideband mode has 99.9% fidelity

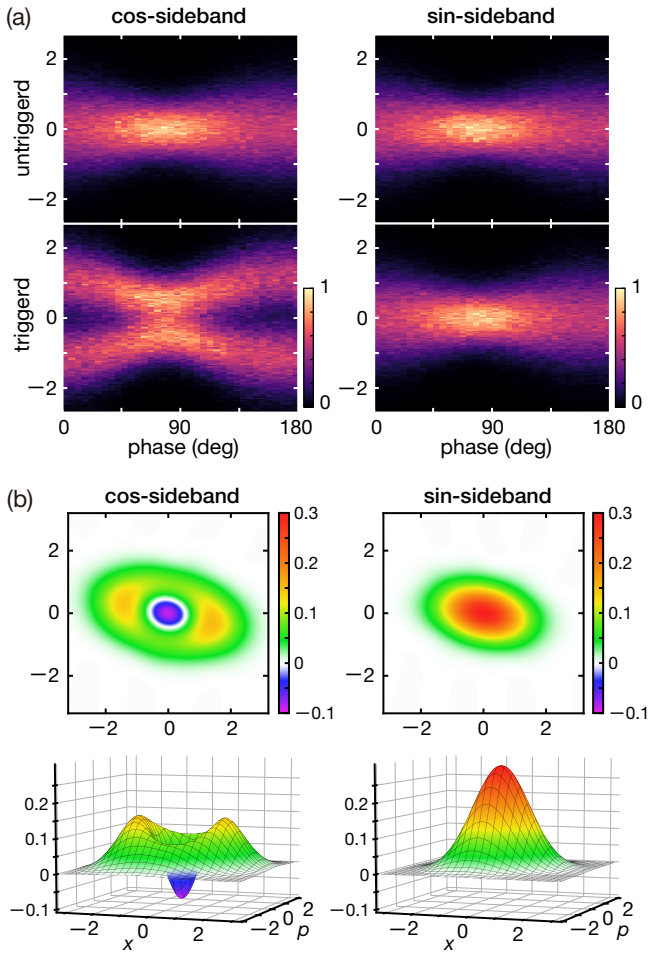

FIG. 4. (a) Quadrature distributions of 36 phase slices ($\hbar = 1$). Upper row: recorded regardless of trigger. Lower row: triggered. (b) Reconstructed Wigner functions. This is directly observed data and no analytical corrections for experimental imperfections are applied.

to the lossy squeezed state since it is untouched by the subtraction. There are no extra factors that limit the purity in our method than the conventional photon subtraction; the major imperfection is the detection efficiency which is relatively low compared to the baseband experiments [36]. Our work can be compared with the recent works by Averchenko *et al.* [37] and Ra *et al.* [38], where they suggest and demonstrate pulse shaping of photon subtractors by means of gate pulses and frequency up-conversion. In their method, however, higher-order sideband modes have complex pulse shapes so as to achieve orthogonality, and it gradually gets difficult to actually use such higher frequency modes.

In conclusion, we have proposed and experimentally realized a highly pure photon subtractor that operates on high-frequency sideband modes of light. The target DSB mode is suitable to the frequency-division multiplexing of non-Gaussian states. Our scheme is applied to the creation of a cat state on a 500 MHz sideband with about 5 MHz of bandwidth and negativity in the Wigner function is observed. Our techniques developed here can be applied to higher order sidebands of the OPO just by changing the frequency of the phase modulation, while keeping the time-domain shape of the envelope. With an LO light at 0 Hz, any DSB modes at various frequencies can be simultaneously measured in principle [39]. In addition to such multi-frequency encoding, it is notable that two quadrature sideband modes (sin and cos) at one frequency are also useful for dual-rail encoding of quantum states. By shifting the modulation phase θ, our method becomes a non-local photon subtraction over the sin- and cos-modes, leading to production of an entangled state between cat states and squeezed states. Also, since the DSB encoding (cos- and sin-sideband modes) and single-sideband encoding (upper- and lower-sideband modes) are connected by effective beamsplitter transformations, these encoding can be used for single-beam implementations of quantum teleportation [40] or cat breeding protocols [41].

This work was supported by CREST (JPMJCR15N5) of JST, JSPS KAKENHI, and the Australian Research Council Centre of Excellence for Quantum Computation and Communication Technology (Project No. CE170100012).

* akiraf@ap.t.u-tokyo.ac.jp

[1] J. Zhang and S. L. Braunstein, Phys. Rev. A **73**, 032318 (2006).
[2] S. Yokoyama, R. Ukai, S. C. Armstrong, C. Sornphiphatphong, T. Kaji, S. Suzuki, J. Yoshikawa, H. Yonezawa, N. C. Menicucci, and A. Furusawa, Nature Photonics **7**, 982 (2013).
[3] M. Pysher, Y. Miwa, R. Shahrokhshahi, R. Bloomer, and O. Pfister, Phys. Rev. Lett. **107**, 030505 (2011).
[4] M. Chen, N. C. Menicucci, and O. Pfister, Phys. Rev. Lett. **112**, 120505 (2014).
[5] R. Raussendorf and H. J. Briegel, Phys. Rev. Lett. **86**, 5188 (2001).
[6] N. C. Menicucci, P. van Loock, M. Gu, C. Weedbrook, T. C. Ralph, and M. A. Nielsen, Phys. Rev. Lett. **97**, 110501 (2006).
[7] S. Lloyd and S. L. Braunstein, Phys. Rev. Lett. **82**, 1784 (1999).
[8] R. Filip, P. Marek, and U. L. Andersen, Phys. Rev. A **71**, 042308 (2005).
[9] M. Dakna, T. Anhut, T. Opatrný, L. Knöll, and D.-G. Welsch, Phys. Rev. A **55**, 3184 (1997).
[10] M. S. Kim, J. Phys. B **41**, 133001 (2008).
[11] A. Zavatta, J. Fiurášek, and M. Bellini, Nature Photonics **5**, 52 (2011).
[12] C. Navarrete-Benlloch, R. García-Patrón, J. H. Shapiro, and N. J. Cerf, Phys. Rev. A **86**, 012328 (2012).
[13] T. J. Bartley, P. J. D. Crowley, A. Datta, J. Nunn, L. Zhang, and I. Walmsley, Phys. Rev. A **87**, 022313 (2013).
[14] O. Morin, K. Huang, J. Liu, H. Le Jeannic, C. Fabre, and J. Laurat, Nature Photonics **8**, 570 (2014).
[15] A. Ourjoumtsev, R. Tualle-Brouri, J. Laurat, and P. Grangier, Science **312**, 83 (2006).
[16] J. S. Neergaard-Nielsen, B. M. Nielsen, C. Hettich, K. Mølmer, and E. S. Polzik, Phys. Rev. Lett. **97**, 083604 (2006).
[17] A. Ourjoumtsev, H. Jeong, R. Tualle-Brouri, and P. Grangier, Nature **448**, 784 (2007).
[18] Z. Leghtas, G. Kirchmair, B. Vlastakis, R. J. Schoelkopf, M. H. Devoret, and M. Mirrahimi, Phys. Rev. Lett. **111**, 120501

(2013).
[19] N. Ofek, A. Petrenko, R. Heeres, P. Reinhold, Z. Leghtas, B. Vlastakis, Y. Liu, L. Frunzio, S. Girvin, L. Jiang, *et al.*, Nature **536**, 441 (2016).
[20] T. C. Ralph, A. Gilchrist, G. J. Milburn, W. J. Munro, and S. Glancy, Phys. Rev. A **68**, 042319 (2003).
[21] N. C. Menicucci, S. T. Flammia, and O. Pfister, Phys. Rev. Lett. **101**, 130501 (2008).
[22] S. T. Flammia, N. C. Menicucci, and O. Pfister, Journal of Physics B: Atomic, Molecular and Optical Physics **42**, 114009 (2009).
[23] N. C. Menicucci, Phys. Rev. Lett. **112**, 120504 (2014).
[24] M. Gu, C. Weedbrook, N. C. Menicucci, T. C. Ralph, and P. van Loock, Phys. Rev. A **79**, 062318 (2009).
[25] K. Marshall, R. Pooser, G. Siopsis, and C. Weedbrook, Phys. Rev. A **91**, 032321 (2015).
[26] J. Brendel, N. Gisin, W. Tittel, and H. Zbinden, Phys. Rev. Lett. **82**, 2594 (1999).
[27] S. Takeda, T. Mizuta, M. Fuwa, J. Yoshikawa, H. Yonezawa, and A. Furusawa, Phys. Rev. A **87**, 043803 (2013).
[28] B. Julsgaard, J. Sherson, J. I. Cirac, J. Fiurášek, and E. S. Polzik, Nature **432**, 482 (2004).
[29] J. Capmany and C. R. Fernández-Pousa, J. Opt. Soc. Am. B **27**, A119 (2010).
[30] A. E. Dunlop, E. H. Huntington, C. C. Harb, and T. C. Ralph, Phys. Rev. A **73**, 013817 (2006).
[31] P. Wang, W. Fan, and O. Pfister, arXiv:1403.6631 (2014).
[32] T. Serikawa and A. Furusawa, Rev. Sci. Instrum. **89**, 063120 (2018).
[33] P. Comon, Signal processing **36**, 287 (1994).
[34] A. Lvovsky, J. Opt. B: Quantum Semiclass. Opt. **6**, S556 (2004).
[35] J. Yoshikawa, W. Asavanant, and A. Furusawa, Phys. Rev. A **96**, 052304 (2017).
[36] W. Asavanant, K. Nakashima, Y. Shiozawa, J. Yoshikawa, and A. Furusawa, Opt. Express **25**, 32227 (2017).
[37] V. A. Averchenko, V. Thiel, and N. Treps, Phys. Rev. A **89**, 063808 (2014).
[38] Y.-S. Ra, C. Jacquard, A. Dufour, C. Fabre, and N. Treps, Phys. Rev. X **7**, 031012 (2017).
[39] T. C. Ralph, E. H. Huntington, and T. Symul, Phys. Rev. A **77**, 063817 (2008).
[40] H. Song, H. Yonezawa, K. B. Kuntz, M. Heurs, and E. H. Huntington, Phys. Rev. A **90**, 042337 (2014).
[41] D. V. Sychev, A. E. Ulanov, A. A. Pushkina, M. W. Richards, I. A. Fedorov, and A. I. Lvovsky, Nature Photonics **11**, 379 (2017).
[42] J. Appel, D. Hoffman, E. Figueroa, and A. I. Lvovsky, Phys. Rev. A **75**, 035802 (2007).
[43] B. Efron and R. Tibshirani, Statistical science , 54 (1986).